Eur. J. Mech. B - Fluids 19 (2000) 403–421

S0997-7546(00)00118-7/FLA

Evolution of a vortex in a magnetic field

Binod Sreenivasan *, Thierry Alboussière

Department of Engineering, University of Cambridge, Trumpington Street, Cambridge CB2 1PZ, UK

(Received 18 October 1999; revised 29 February 2000; accepted 2 March 2000)

Abstract – The evolution of a single vortex in an electrically-conducting liquid, subject to a uniform magnetic field acting parallel to the axis of the vortex, is investigated by an order-of-magnitude analysis and a numerical model. The non-linear phase of decay, wherein the Lorentz and the inertial forces are of the same order of magnitude, is studied in detail. As the kinetic energy decays primarily due to Joule dissipation, the vortex evolves in such a way that the component of angular momentum parallel to the direction of the magnetic field is conserved. If the true interaction parameter, N_t, which denotes the actual ratio of the Lorentz to the inertial forces, is assumed to be a constant of order unity in the non-linear regime, the evolution of the vortex can be fully described. The above assumption is proven to be correct not only from the values of N_t obtained in the numerical simulation, but also from the good agreement between the theoretical and numerically-obtained energy decay laws for the non-linear phase, at finite time. In addition, the true interaction parameter proves to be useful in estimating the minimum magnetic field strength required for stable evolution of a swirling vortex.

(KWD) vortex decay / MHD / magnetic field / interaction parameter

1. Introduction

The tendency of flow structures in an electrically conducting fluid, such as a liquid metal, to elongate in the direction of an applied magnetic field has been established from several experiments (Votsish and Kolesnikov [1] and Alemany et al. [2]). The experiments led to the conclusion that correlations are stronger in the direction parallel to the external field. When a magnetic field acts on a three-dimensional velocity field, the velocity gradient in the direction of the magnetic field is reduced by the Lorentz forces, so that the velocity becomes almost independent of the coordinate parallel to the field. Whether a fluid structure becomes two-dimensional or not depends on the presence of solid boundaries transverse to the magnetic field (see Sommeria and Moreau [3]). It is also clear from experiments that the destruction of kinetic energy in the presence of a magnetic field is accelerated by Joule dissipation.

The initial phase of decay of vortices under a strong magnetic field is characterized by dominant Joule dissipation. This 'linear' regime, where inertial effects are negligible, has been studied theoretically in the literature (Moffatt [4], Davidson [5]). In this paper, we study the magnetic damping of an isolated vortex in the subsequent non-linear phase.

An overview of the previous studies on magnetic damping is given in section 2. In these studies and in the present work, the ratio of the Lorentz to the inertial forces, as quantified by the interaction parameter, N, is initially much greater than unity. The ratio of convection to magnetic diffusion, represented by the magnetic Reynolds number, R_m, is much lesser than one. In section 3, an order-of-magnitude analysis of the evolution of an isolated vortex aligned with the external magnetic field is presented. We first consider the principle of conservation of angular momentum as applied to a growing vortex. Then, the ratio of the actual magnitudes

* Correspondence and reprints; e-mail: bs229@eng.cam.ac.uk

of the Lorentz to the inertial forces, referred to as the 'true' interaction parameter, N_t, is studied. Finally, the global kinetic energy equation for the vortex is derived. In the light of earlier experimental spectral studies on magnetically-damped turbulent flows, it is shown that, unlike in conventional turbulence, viscous dissipation cannot contribute significantly to the decay of kinetic energy, and Joule dissipation alone plays the dominant role. The solution of the three governing equations, namely, the angular momentum equation, the energy equation and the law of variation of the true interaction parameter, describes the non-linear vortex evolution. Section 4 is devoted to the numerical investigation of the damping of an axisymmetric vortex that is parallel to the magnetic field. A range of initial interaction parameters are considered, to visualize the effect of the field strength on the evolution pattern. The variation of the true interaction parameter is studied to identify the situation where the inertial and Lorentz forces balance initially. In the concluding section, we comment on the agreement of the numerical results with the ideas developed in 3.

2. Previous studies

As mentioned earlier, the initial phase of decay of a turbulent flow field in a uniform magnetic field has been treated theoretically in the literature, for the case of a high interaction parameter and a low magnetic Reynolds number. The first condition implies that the characteristic time during which a magnetic field eliminates velocity gradients in its direction, the Joule time (τ), is small in comparison with the turn-over time of an eddy, $t_0 (= l/u)$:

$$\tau = \rho/\sigma B^2 \ll l/u, \tag{1}$$

where ρ and σ are the density and electrical conductivity of the fluid, l and u are the typical size and velocity of the vortex, and **B** is the magnetic flux density, so that the interaction parameter, N, is large compared to unity:

$$N = t_0/\tau = \sigma B^2 l/\rho u \gg 1. \tag{2}$$

The condition of low magnetic Reynolds number means that the distortion of the imposed magnetic field by the velocity field is negligible because diffusion of the field dominates over convection.

$$R_m = ul/\eta \ll 1, \tag{3}$$

where η is the magnetic diffusivity.

Moffatt [4] studied the decay of the fourier transform of the linearised, inviscid equation of motion for $\tau < t < N_0\tau$. The turbulent kinetic energy decays as $(t/\tau)^{-1/2}$. The turbulence was described as two-dimensional, in the sense that all quantities vary slowly in the direction parallel to **B** compared with their variation perpendicular to **B**.

Sommeria and Moreau [3] expressed the electromagnetic force in the equation of motion in a form resembling a uni-directional diffusion term. By including the irrotational part of the $\mathbf{j} \times \mathbf{B}$ force in the pressure, the equation of motion becomes:

$$\frac{\mathrm{D}\mathbf{u}}{\mathrm{D}t} = -\frac{1}{\rho}\nabla_\perp p^* + \nu\nabla_\perp^2\mathbf{u} - \frac{\sigma B^2}{\rho}\nabla_\perp^{-2}\left(\frac{\partial^2\mathbf{u}}{\partial z^2}\right), \tag{4}$$

where p^* is the augmented pressure and ∇^{-2} is the inverse of the Laplacian operator. Assuming that the applied field is in the z-direction, the subscript '$\perp$' is defined in a transverse (x, y) plane. This is valid because the gradient in the z-direction becomes small in comparison with that in the other two directions, as a vortex

elongates. The vorticity equation can be written in the following approximate 'linear' form when both N_0 and Re are large:

$$\frac{\partial \omega}{\partial t} = -\frac{\sigma B^2}{\rho} \nabla_{\perp}^{-2} \left(\frac{\partial^2 \omega}{\partial z^2} \right). \tag{5}$$

The application of the $\nabla_{\perp}^{-2}$ operator is equivalent to multiplication by $(-l_{\perp}^2)$ in Fourier space, where $l_{\perp}$ is the length scale perpendicular to the field. The term on the right of (5) is, therefore, a pseudo-diffusion term along **B**, $(l_{\perp}^2/\tau)\partial^2\omega/\partial z^2$. In short, the elongation of a vortex is a manifestation of the diffusion of vorticity along the **B**-lines. The length scale parallel to the field, $l_{\parallel}$, is expected to evolve at a rate

$$l_{\parallel} = l_{\perp}(t/\tau)^{1/2}. \tag{6}$$

From the above relation, Sommeria and Moreau [3] suggested that, during the typical turn-over time, l/u, of a turbulent structure subject to a magnetic field, an anisotropic state is attained wherein

$$l_{\parallel}/l_{\perp} \sim N^{1/2}, \tag{7}$$

if $l_{\perp}N^{1/2}$ is smaller than the spacing of the walls perpendicular to the applied field.

Davidson [5] used the classical result in electromagnetism that any closed current loop situated in a uniform magnetic field experiences a resultant magnetic torque, **T**, perpendicular to **B**. It was shown that the component of **T** parallel to **B**, integrates to zero over a volume that is either infinite in extent or else bounded by an electrically-insulating surface. The fluid domain may be considered to be made up of several such infinitesimal current paths, each forming a closed loop. In short, the Lorentz force cannot affect the component of angular momentum parallel to **B**, $\mathbf{H}_{\parallel}$. If $l_{\perp}$ is assumed to be unaffected by the field during the initial phase of evolution, the condition of constant $\mathbf{H}_{\parallel}$ can be coupled with the energy equation to give the laws of evolution of energy and the parallel length scale obtained by Moffatt [4] and Sommeria and Moreau [3].

3. Evolution of an isolated vortex: the governing equations

In this section, we perform an order-of-magnitude analysis of the evolution of a vortex whose axis is parallel to the direction of a uniform, static magnetic field, in a quiescent liquid metal. The fluid domain, V, is infinite in extent, or the electrically-insulating boundaries are far from the initial location of the vortex, so that their effect is not felt in the evolution process.

The laws of angular momentum conservation and energy decay are obtained. A relationship between the length scales also needs to be derived to account for the non-linear effects.

3.1. Conservation of angular momentum

Since all current paths close within the volume, the law of conservation of $\mathbf{H}_{\parallel}$ becomes applicable. The global angular momentum is defined as

$$\mathbf{H} = \rho \int_V \mathbf{x} \times \mathbf{u} \, \mathrm{d}V. \tag{8}$$

The density, ρ, being constant and uniform, the conservation of $\mathbf{H}_{\parallel}$ can be written as follows:

$$E^{1/2} l_{\perp}^2 l_{\parallel}^{1/2} = E_0^{1/2} l_0^{5/2} = \text{const.}, \tag{9}$$

where E_0 is the initial kinetic energy, l_0 is the initial length scale of the vortex and $E \sim \int_V u^2 \, \mathrm{d}V$. The above equation is valid throughout the period of evolution of a vortex, and also for any value of the initial interaction parameter, denoted by N_0.

3.2. The 'true' interaction parameter

The laws governing the evolution of a vortex in the initial phase can be derived easily because $l_\perp$ is assumed to remain unaffected by the Joule effect at large N. But during the elongation process of a vortex, the current density falls so that the inertial forces become significant at some stage. It would be erroneous to assume that $l_\perp$ is a constant during non-linear evolution. The definition of the true interaction parameter, N_t, gives additional information about the evolution in this phase. N_t is the ratio of the actual magnitudes of the Lorentz to the inertial forces. Estimating the rotational part of the Lorentz force, **F**, from equation (4), we obtain

$$\frac{\operatorname{curl}\mathbf{F}}{\operatorname{curl}[\rho(\mathbf{u}\cdot\nabla)\mathbf{u}]} \sim \frac{\sigma B^2 l_\perp}{\rho u}\left(\frac{l_\perp}{l_\parallel}\right)^2 \sim N\left(\frac{l_\perp}{l_\parallel}\right)^2, \tag{10}$$

where N is the nominal interaction parameter. From the known estimates of the decay of kinetic energy and the growth of the parallel length scale of a vortex during the initial linear phase of evolution, $E \sim (t/\tau)^{-1/2}$ and $l_\parallel \sim (t/\tau)^{1/2}$, the nominal interaction parameter is given by the estimate

$$N \sim N_0 (t/\tau)^{1/2}, \tag{11}$$

and hence, the true interaction parameter is defined by

$$N_t = N\left(\frac{l_\perp}{l_\parallel}\right)^2 \sim N_0 (t/\tau)^{-1/2}. \tag{12}$$

N_t decreases as a function of time, and when $t \sim N_0^2\tau$, $\operatorname{curl}(\mathbf{j}\times\mathbf{B})$ falls to the same order of magnitude as $\operatorname{curl}[\rho(\mathbf{u}\cdot\nabla)\mathbf{u}]$, and the problem becomes non-linear. At the end of the so-called linear phase,

$$N_t = N\left(\frac{l_\perp}{l_\parallel}\right)^2 = \frac{l_\perp^2 l_\parallel^{1/2}}{\tau E^{1/2}}\left(\frac{l_\perp}{l_\parallel}\right)^2 \sim 1. \tag{13}$$

We make the assumption that N_t remains a constant of order unity during the non-linear evolution. The above relation is also obtained from the order-of-magnitude relationship (7) put forward by Sommeria and Moreau [3].

The duration of the initial linear phase of magnetic damping is obtained directly from the definition of N_t. The duration of the linear phase during the damping of an isolated vortex is $N_0^2\tau$, because the global kinetic energy, E, decays as $(t/\tau)^{-1/2}$. However, in the context of MHD turbulence, where the kinetic energy per unit mass of the turbulence is given by the mean square value of the velocity, $\overline{u^2}$, a similar order-of-magnitude calculation tells us that this phase lasts up to $N_0^{4/3}\tau$. Alemany et al. [2] had obtained the latter result for MHD turbulence from spectral arguments.

If $N_0 \gg 1$, the true interaction parameter of a vortex is expected to tend asymptotically to unity regardless of its initial value. If the inertial and Lorentz forces balance, N_t will be a constant of order one in the presence of a steady applied magnetic field as neither Lorentz nor the inertial force gains the upper hand during the evolution process. If, on the other hand, $N_0 \ll 1$, the vortex experiences only weak Joule dissipation initially. Davidson

[5] had predicted that the angular momentum would rearrange itself into rings that propagate radially outward. In this paper, we shall identify the value of N_0 below which such a phenomenon is likely to happen.

3.3. The energy equation

The rate of decay of the global kinetic energy, $\int_V u^2 \, \mathrm{d}V$ can be expressed as

$$\frac{\mathrm{d}E}{\mathrm{d}t} = -\varepsilon - D, \tag{14}$$

where ε and D are the viscous and Joule dissipation rates per unit mass, respectively. Of these, the Joule dissipation is expressed as

$$D = \int_V \frac{\mathbf{j}^2}{\rho\sigma} \, \mathrm{d}V. \tag{15}$$

From Ohm's law in the form

$$\operatorname{curl} \mathbf{j} = \sigma \operatorname{curl}(\mathbf{u} \times \mathbf{B}) = \sigma (\mathbf{B} \cdot \nabla)\mathbf{u}, \tag{16}$$

for a spatially-uniform field, the following estimates of the current, and hence the Joule dissipation can be derived:

$$\begin{aligned} \mathbf{j} &\sim \sigma B \mathbf{u} \left(\frac{l_\perp}{l_\parallel} \right), \\ D &\sim \frac{\sigma B^2}{\rho} \left(\frac{l_\perp}{l_\parallel} \right)^2 \int_V u^2 \, \mathrm{d}V \sim \frac{E}{\tau} \left(\frac{l_\perp}{l_\parallel} \right)^2. \end{aligned} \tag{17}$$

The order of magnitude of the viscous dissipation term, ε, in the energy equation (14) can also be estimated for the non-linear decay phase. This is necessary because the vortex can be turbulent and could contain an energy cascade, leading to significant viscous dissipation. In conventional turbulence, the energy spectrum, $E(k)$ in the inertial subrange varies as $k^{-5/3}$. In the spectra obtained experimentally for liquid metal flows in a magnetic field, the inertial range is found to have a slope of -3 instead of the Kolmogorov slope of $-5/3$. Kolesnikov and Tsinober [6] studied the spectra of longitudinal velocity fluctuations in turbulent flow of mercury in the wake behind a cylinder aligned parallel to a magnetic field. While a slope of $-5/3$ was observed for the inertial range under weak fields, a clear slope of -3 was found for flow in a strong magnetic field ($N_0 \geqslant 8$). In a continuation of the above study, Votsish and Kolesnikov [1] measured the intensities of velocity and vorticity fluctuations in turbulent flow of mercury in a rectangular channel with non-conducting walls. The spectra of energy and enstrophy presented slopes of -3 and -1 respectively. Alemany et al. [2] investigated experimentally the case when the initial interaction parameter took low (~ 0.1) as well as moderate (~ 1) values. Their configuration consisted of a grid moving through a vertical column of mercury subjected to an axial, homogeneous DC magnetic field. They observed an increase in the integral length scale parallel to **B**. The experiments were quite different from those performed earlier, because the measurements were free from the influence of the boundaries. The one-dimensional spectrum obtained based on the longitudinal velocity correlation has a well-defined $k_\parallel^{-3}$ range. The k^{-3} spectrum was explained in terms of an equilibrium between the Joule dissipation and the energy transport from the energy-containing zone to the dissipation zone in Fourier space. In a later study conducted in Beer Sheva, Sukoriansky et al. [7] obtained experimental spectra that clearly displayed a slope of -3 in the high wave number range.

If k_0 is the wave number corresponding to the large (energy-containing) scales, the large wavenumber spectral kinetic energy density in MHD can thus be written as

$$E(k) = E(k_0)\left(\frac{k}{k_0}\right)^{-3}, \tag{18}$$

and the spectral Reynolds number, $Re(k)$, is given by

$$Re(k) = \frac{u}{\nu k} = \frac{[E(k_0)]^{1/2}}{\nu}\frac{k_0^{3/2}}{k^2}, \tag{19}$$

where $u \sim [kE(k)]^{1/2}$. If we impose the condition that the Reynolds number corresponding to the smallest scales, $Re(k_{\max})$ is of order unity, then

$$\frac{k_{\max}}{k_0} \sim \left[Re(k_0)\right]^{1/2}. \tag{20}$$

The kinetic energy, E, and the viscous dissipation rate, ε can be approximated by (see Hinze [8])

$$\begin{aligned} E &\approx \int_{k_0}^{k_{\max}} E(k)\,\mathrm{d}k \sim k_0 E(k_0), \\ \varepsilon &\approx 2\nu \int_{k_0}^{k_{\max}} k^2 E(k)\,\mathrm{d}k \sim \nu k_0^3 E(k_0)\ln Re(k_0) \sim E\nu k_0^2 \ln Re(k_0). \end{aligned} \tag{21}$$

If a $k^{-5/3}$ spectrum had been chosen, then the viscous dissipation would have been estimated by the following expressions:

$$E\nu k_0^2 Re(k_0) \sim u^3/l_0. \tag{22}$$

Now, the Joule dissipation, D, (given by equation (17), but with $E \sim \overline{u^2}$) is also of order u^3/l_0 if we take into account the condition laid down by the relation (13). Therefore, the first expression in (22) becomes an apt estimate for D. Hence, the ratio of viscous to Joule dissipation rate in MHD turbulence is given by

$$\frac{\varepsilon}{D} \sim \frac{\ln[Re(k_0)]}{Re(k_0)}. \tag{23}$$

At high Reynolds numbers, ε/D is very small, implying that viscous damping is negligible in comparison with ohmic damping even in the turbulent regime, and relation (17) is a sound estimate for the energy decay rate throughout the evolution process.

3.4. Decay of kinetic energy and growth of anisotropy

If the inertial and Lorentz forces acting on a vortex are approximately of the same magnitude, it will evolve in such a way that the true interaction parameter is a constant of order one throughout the decay process (until the growth of the vortex is influenced by the presence of solid boundaries). The equations governing the evolution of the vortex have been developed in the previous sections. They are the equation of conservation of angular momentum, the energy decay equation and the condition of the true interaction parameter being of order unity.

$$E^{1/2} l_\perp^2 l_\parallel^{1/2} = \text{const.}, \tag{24}$$

$$\frac{\mathrm{d}E}{\mathrm{d}t} \sim -\frac{E}{\tau}\left(\frac{l_\perp}{l_\parallel}\right)^2, \tag{25}$$

$$N_t = \frac{l_\perp^2 l_\parallel^{1/2}}{\tau E^{1/2}}\left(\frac{l_\perp}{l_\parallel}\right)^2 \sim 1. \tag{26}$$

From the above equations, the following laws for the decay of kinetic energy and the evolution of the length scales can be derived for the non-linear phase ($t > N_0^2\tau$):

$$\frac{E}{E_0} \sim \left[1 + \frac{1}{N_0}(t/\tau)\right]^{-1}, \tag{27}$$

$$\frac{l_\parallel}{l_0} \sim N_0^{2/5}\left[1 + \frac{1}{N_0}(t/\tau)\right]^{3/5}, \tag{28}$$

$$\frac{l_\perp}{l_0} \sim N_0^{-1/10}\left[1 + \frac{1}{N_0}(t/\tau)\right]^{1/10}. \tag{29}$$

When $t \sim N_0^2\tau$, the initial conditions that correspond to the end of the linear phase are recovered:

$$E/E_0 \sim 1/N_0, \qquad l_\parallel/l_0 \sim N_0, \qquad l_\perp \approx l_0. \tag{30}$$

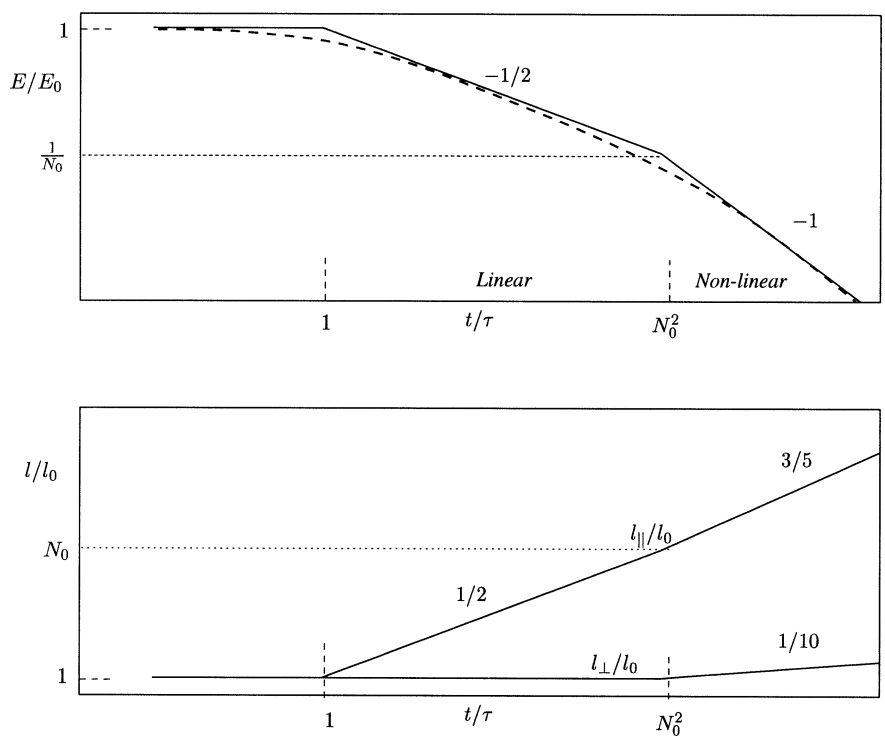

Figure 1. Overall evolution of kinetic energy and length scales of a single vortex, at large N_0, in logarithmic scales.

At large times, the following behaviour is obtained:

$$E \sim (t/\tau)^{-1}, \qquad l_{\parallel}/l_{\perp} \sim (t/\tau)^{1/2}. \tag{31}$$

The global evolution of E, $l_{\parallel}$ and $l_{\perp}$ at large N_0, including the linear and non-linear regimes, is shown schematically in *figure 1*. The dotted curve is a typical representation of the decay of kinetic energy of the vortex.

4. Numerical simulation of the evolution of an aligned vortex

The case of a vortex whose axis is aligned with the direction of the magnetic field, **B** is considered numerically in this section. Suppose we have a localized region of swirl in an otherwise quiescent liquid metal. We assume the flow structure to be axisymmetric, whereby the velocity field is independent of θ in the cylindrical co-ordinate system (r, θ, z). This swirling vortex is situated in a magnetic field pointing in the z-direction.

4.1. Governing equations

For a θ-independent velocity field, the full Navier–Stokes equations in cylindrical polar co-ordinates with the Lorentz force terms in them are

$$\frac{\partial \Gamma}{\partial t} + (\mathbf{u}_p \cdot \nabla)\Gamma = -\frac{1}{\tau}\nabla_*^{-2}\left(\frac{\partial^2 \Gamma}{\partial z^2}\right) + \nu \nabla_*^2 \Gamma, \tag{32}$$

$$\frac{\partial u_r}{\partial t} + (\mathbf{u}_p \cdot \nabla)u_r = -\frac{1}{\rho}\frac{\partial p}{\partial r} + \frac{1}{r^3}\Gamma^2 - \frac{u_r}{\tau} + \nu\left(\nabla^2 u_r - \frac{u_r}{r^2}\right), \tag{33}$$

$$\frac{\partial u_z}{\partial t} + (\mathbf{u}_p \cdot \nabla)u_z = -\frac{1}{\rho}\frac{\partial p}{\partial z} + \nu \nabla^2 u_z, \tag{34}$$

$$\frac{1}{r}\frac{\partial \Gamma}{\partial r} + \frac{\partial u_z}{\partial z} = 0, \tag{35}$$

where Γ is the local angular momentum, ru_θ and $\mathbf{u}_p = (u_r, u_z)$. The operator ∇_*^2 is given by

$$\nabla_*^2 f = r\frac{\partial}{\partial r}\left(\frac{1}{r}\frac{\partial f}{\partial r}\right) + \frac{\partial^2 f}{\partial z^2}. \tag{36}$$

∇_*^{-2} is the inverse of the above operator, equivalent to an integration process in the (r, z) plane. The Lorentz terms on the right hand sides of equations (32) and (33) are obtained by considering the interaction of u_θ and u_p with **B** (see Davidson [5] for the development). We see that all electric current paths in the azimuthal plane form closed loops. The electric current in the poloidal (r, z) plane is expressed in terms of a stream function, ξ, so that

$$\mathbf{j}_p = \sigma B\left[\nabla \times (\xi/r)\mathbf{e}_\theta\right], \tag{37}$$

and, by virtue of equation (16),

$$\nabla_*^2 \xi = -\partial \Gamma/\partial z. \tag{38}$$

Equations (33) and (34) can be re-written in terms of the azimuthal vorticity by evaluating their curl:

$$\frac{\partial}{\partial t}\left(\frac{\omega_\theta}{r}\right) + (\mathbf{u}_p \cdot \nabla)\frac{\omega_\theta}{r} = \frac{1}{r^4}\frac{\partial}{\partial z}\Gamma^2 - \frac{1}{r^2\tau}\frac{\partial^2}{\partial z^2}\left[\nabla_*^{-2}(r\omega_\theta)\right] + \nu\left[\nabla^2\left(\frac{\omega_\theta}{r}\right) + \frac{2}{r}\frac{\partial}{\partial r}\left(\frac{\omega_\theta}{r}\right)\right]. \tag{39}$$

The Lorentz term is expressed in the form given in equation (39) by noting

$$u_r = -\frac{1}{r}\frac{\partial\psi}{\partial z}, \qquad u_z = \frac{1}{r}\frac{\partial\psi}{\partial r}, \qquad \nabla_*^2\psi = -r\omega_\theta, \tag{40}$$

where ψ is the stream function for u_p. The first term on the right hand side of equation (39) represents the generation of ω_θ by the axial gradient in Γ (due to differential rotation of the vortex).

Pumir and Siggia [9] have studied the evolution of axisymmetric vortices with swirl. The undamped Euler equations were solved using a finite-difference method, to show that, when $\nu = 0$, the gradients in ω_θ become infinite at finite time, resulting in a singularity. In a later work, Grauer and Sideris [10] presented computational evidence for the occurrence of a finite-time singularity in the axisymmetric Euler equations, with two different numerical schemes.

4.2. Numerical method

We solve equations (32) and (39) numerically to study the evolution of a parallel vortex in a magnetic field. At time $t = 0$, the Γ-distribution is assumed to be

$$\Gamma_0(r, z) = r^2 \mathrm{e}^{-(r^2+z^2)/\delta^2}, \tag{41}$$

where δ is the characteristic decay length in the r and z directions. The initial velocity distribution is assumed to be purely azimuthal, so that $\omega_\theta = 0$ at $t = 0$. The flow field is resolved spectrally by expressing Γ and ψ as Fourier–Bessel series. The transformation is

$$\begin{aligned}\Gamma &= \sum_{m=0}^{M}\sum_{n=1}^{N}\hat{\Gamma}_{mn}\cos(m\pi x)\, y J_1(\delta_n y),\\ \psi &= \sum_{m=1}^{M}\sum_{n=1}^{N}\hat{\psi}_{mn}\sin(m\pi x)\, y J_1(\delta_n y),\end{aligned} \tag{42}$$

$$\begin{aligned}\hat{\Gamma}_{mn} &= \frac{2}{J_0^2(\delta_n)}\int_{x=0}^{1}\int_{y=0}^{1}\Gamma(x, y)\cos(m\pi x) J_1(\delta_n y), \quad m = 0,\\ &= \frac{4}{J_0^2(\delta_n)}\int_{x=0}^{1}\int_{y=0}^{1}\Gamma(x, y)\cos(m\pi x) J_1(\delta_n y), \quad m > 0,\\ \hat{\psi}_{mn} &= \frac{4}{J_0^2(\delta_n)}\int_{x=0}^{1}\int_{y=0}^{1}\psi(x, y)\sin(m\pi x) J_1(\delta_n y),\end{aligned} \tag{43}$$

where δ_n are the zeroes of $J_1(x)$ and $x = z/L$, $y = r/R$, $L = R = 5\delta$. We imagine an isolated vortex of radius 1 cm situated at the centre of a cavity of dimension 10 cm $\times$ 10 cm. The choice of a cosine series for Γ ensures

that $\partial\Gamma/\partial z = 0$ at $z = L$, so that, by equations (37) and (38), there is no flux of the poloidal current across the boundaries. The Lorentz term in equation (32) also vanishes. This is a necessary boundary condition for conservation of angular momentum.

Using the transformation in (42) and (43), equations (32) and (39) are written in spectral form. The Lorentz and the viscous terms decay exponentially in spectral space. A spectral resolution of 30×30 modes is used in the computation. From the point of view of visualizing the effect of the field strength on the evolution of the flow and studying the length scale and energy decay characteristics, this resolution is found to be adequate. A fourth-order Runge–Kutta scheme with adaptive step-size control is used for time-stepping the equations.

The properties of mercury are used in all our numerical runs: $\nu = 1.144 \times 10^{-7}$, $\sigma = 1.04 \times 10^{6}$, $\rho = 13.55 \times 10^{3}$, all in SI units. The initial Reynolds number is 5700.

4.3. Numerical results

In all numerical runs, $\int \Gamma \, \mathrm{d}V$ is found to be a robust invariant. The maximum variation observed is only 1.3% of the initial value, for $N_0 \approx 0.1$. This shows that the boundary conditions on the current are satisfied throughout a run. The following quantities are calculated during each numerical run:

(1) Global kinetic energy per unit mass

$$E = \int_V (u_\theta^2 + u_r^2 + u_z^2) \, \mathrm{d}V. \tag{44}$$

The azimuthal and poloidal energies are also known separately.

(2) Parallel and transverse length scales, $l_\parallel$ and $l_\perp$. To obtain these, we define a correlation coefficient for the Γ-distribution in the (r, z) plane. For instance,

$$c_\parallel(l) = \frac{\sum_{r,z} \Gamma(r,z)\Gamma(r,z+l)}{\sum_{r,z}[\Gamma(r,z)]^2}, \quad 0 < l < L, \tag{45}$$

where l is a shift in the axial direction, so that

$$l_\parallel \sim \left[1/\ddot{c}_\parallel(0)\right]^{1/2}, \tag{46}$$

where $\ddot{c}_\parallel(0)$ is the curvature of the curve $c_\parallel(l)$ at $l = 0$. $l_\perp$ is estimated in a similar fashion, but by shifting the Γ-matrix in the radial direction.

(3) The true interaction parameter, N_t, given by relation (10). The characteristic velocity u used in this relation is given by $\left(E/l_\perp^2 l_\parallel\right)^{1/2}$. The numerical values of N_t quoted in this paper are determined by the values of the length scales obtained by the correlation method explained above.

We begin the study with interaction parameters of order unity. *Figures 2* and *3* show the evolution of the flow structure when N_0 is relatively large (0.8), but still of order one. One-half of the vortex, in the region $-L < z < L, 0 < r < R$, is shown. As time progresses, the swirl motion of the vortex propagates along z. There are no visible non-linear effects. *Figure 3(a)* shows the lines of constant Γ with the lines of constant electric current stream function, ξ superposed on them. The currents that emerge from the vortex interact with the field, creating swirl in previously static regions of the fluid. The same currents circulate back into the vortex, creating an oppositely-signed torque in an annular region surrounding the vortex. This explains the region of negative Γ seen radially ahead of the vortex, in *figures 3* to *6*. The depression observed in the three-dimensional

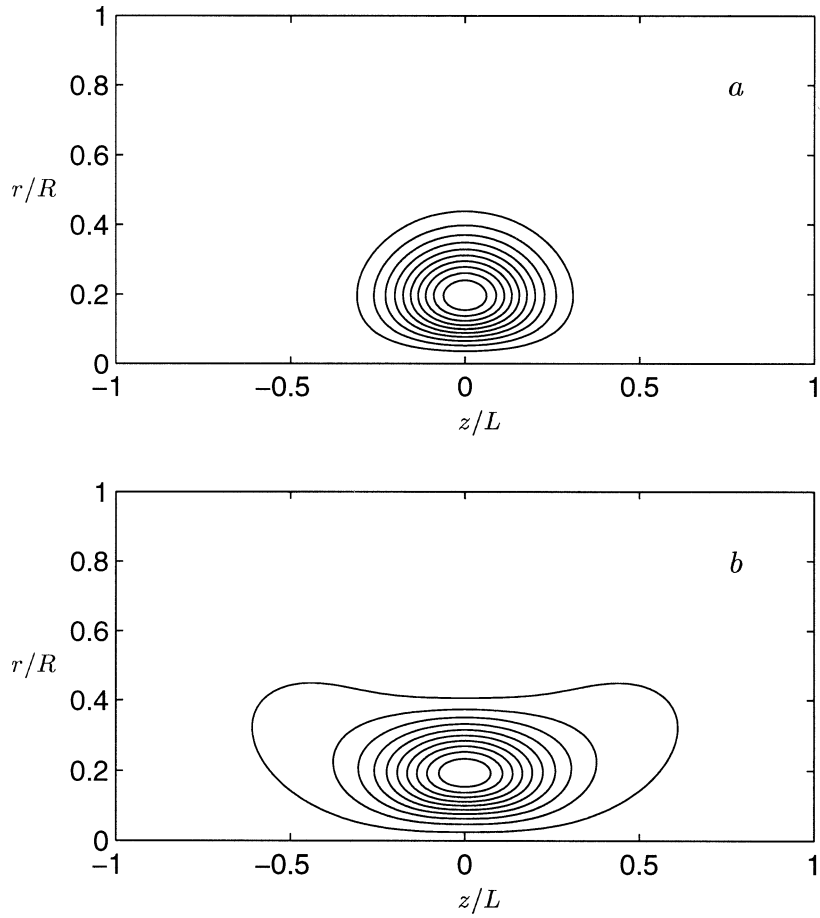

Figure 2. Contour plots of the Γ-field at $N_0 = 0.8$: (a) when $t/\tau = 0$, $\Gamma_{\max} = 3.2 \times 10^{-4}$ at $r = 0.2R$, and Γ decreases to 3.2×10^{-5} at the outer contour; (b) when $t/\tau = 1.0$, $\Gamma_{\max} = 2.5 \times 10^{-4}$ at $r = 0.2R$, $\Gamma = 1.01 \times 10^{-5}$ at the outer contour. Γ values are in m^2s^{-1}.

plot of the Γ distribution in *figure 3(b)* makes this clear. When $N_0 = 0.5$, the evolution is similar, in that, the elongation of the vortex along z is still the dominant mechanism (*figure 4*).

When the field strength is reduced ($N_0 = 0.3$), there are distinct inertial effects. The base of the vortex is indented, and the Γ-lines in the core of the vortex curve inwards, as seen in *figure 5*. From a study of the length scales, we shall see that, while Γ diffuses along the **B**-lines, there is also a displacement in the radial direction. For a weaker magnetic field ($N_0 = 0.12$), the powerful inertial forces transform the vortex into a ring, the cross-section of which is a mushroom-shaped structure, with a cleaved base (*figure 6(a)*) and a shell where the maximum angular momentum gets concentrated (*figure 6(b)*). This region of maximum Γ pushes radially outward from $r = 0.2R$ at $t = 0$ to $r = 0.4R$ at $t = 5\tau$. Pumir and Siggia [9] have predicted a similar kind of behaviour from the analogy between axisymmetric, but undamped swirling flows and buoyancy-driven flows.

Smaller blobs of positive angular momentum are seen radially ahead of the region of reverse flow, at low interaction parameters (in *figures 5* and *6*). These can be attributed to numerical oscillations caused by the high radial gradients in Γ developing at the front end of the vortex. The presence of these oscillations, however, does not affect our physical understanding of the behaviour of a vortex under weak magnetic fields.

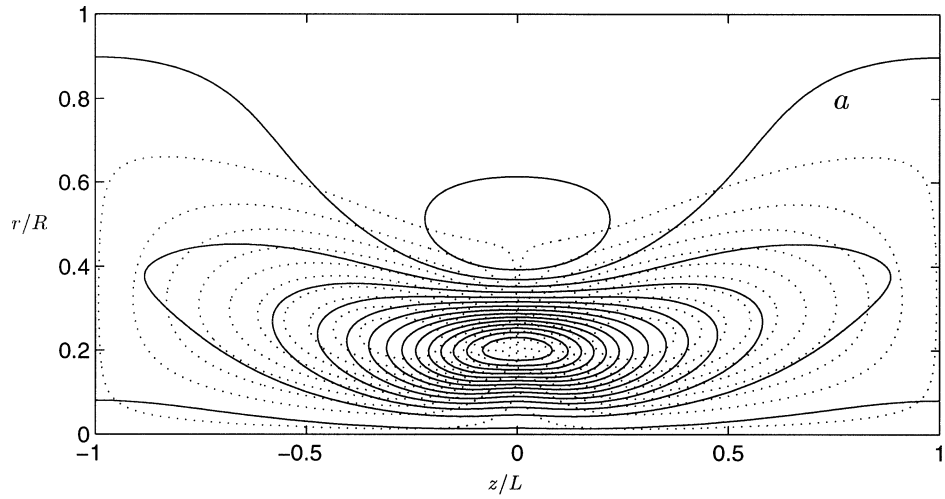

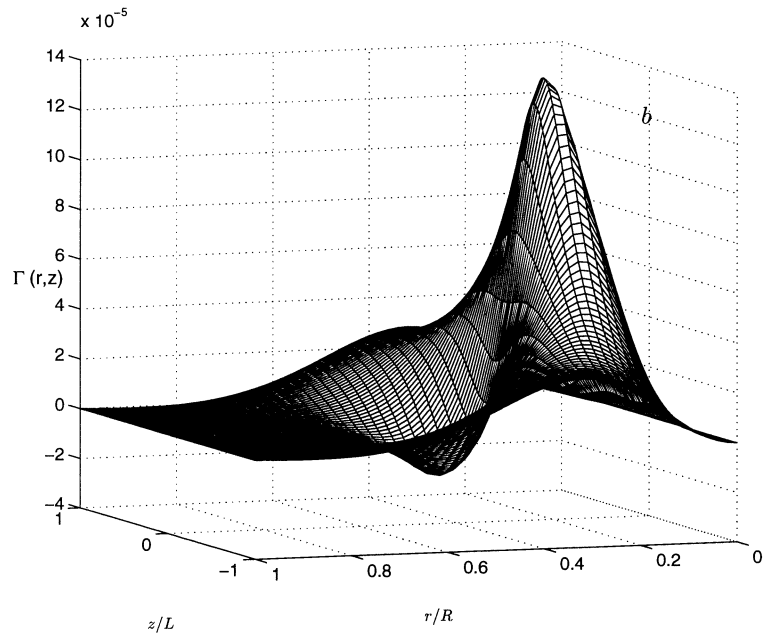

Figure 3. Continuation of *figure 2*: (a) contour plot of the Γ-field when $t/\tau = 3.5$, $\Gamma_{\max} = 1.77 \times 10^{-4}$ at $r = 0.2R$ and $\Gamma = 1.6 \times 10^{-6}$ at the outer contour. A zone of negative angular momentum, with $\Gamma = -1.18 \times 10^{-6}$ is seen ahead of the vortex. The constant ξ-lines (dotted) are superposed. $\xi = -1.48 \times 10^{-7}$ at the core of the vortex, and -1.46×10^{-9} at the outer contour; (b) three-dimensional plot for $t/\tau = 8.0$. $\Gamma_{\max} = 1.28 \times 10^{-4}$ at $r = 0.2R$. The region of negative Γ (wherein $\Gamma = -1.04 \times 10^{-5}$), produced by recirculating currents can be seen as a depression. Γ values are in $m^2 s^{-1}$ and ξ in $m^3 s^{-1}$.

When $z > 0$, $\omega_\theta > 0$, and when $z < 0$, $\omega_\theta < 0$. In the absence of a magnetic field, this vortex dipole will move forward radially. Γ would eventually rise to a high value in the shell region so that $\partial\Gamma/\partial r$ tends to infinity at the front end. In the presence of a strong-enough magnetic field, the above phenomenon is arrested, and only the axial diffusion of Γ dominates. On the other hand, with a very weak field, the eddy turn-over time is sufficiently smaller than the Joule time, so that the vortex is initially subject to the above mentioned centrifugal instability. The evolution is along the same lines for $N_0 = 0.3$ and $N_0 = 0.12$. It is seen from *figure 6* that, in the presence of

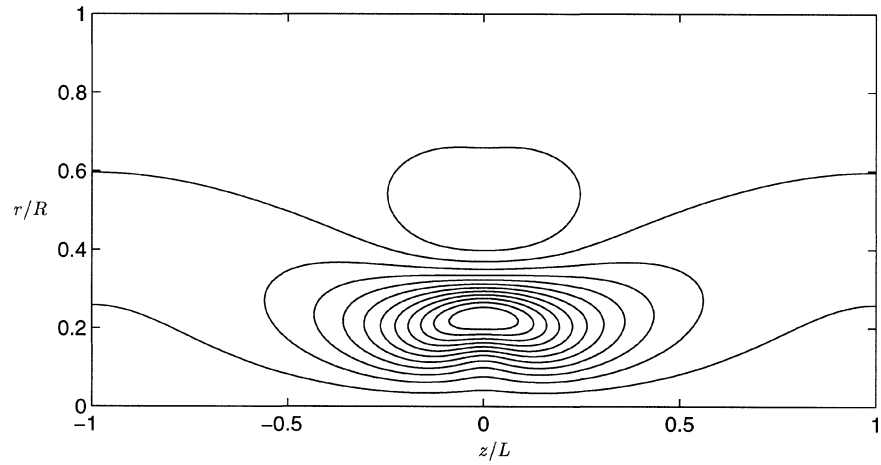

Figure 4. The state of the vortex in *figure 2(a)* after three Joule times, when $N_0 = 0.5$. $\Gamma_{\max} = 1.87 \times 10^{-4}$ at the core of the vortex and $\Gamma = 9.0 \times 10^{-6}$ at the outer contour of the vortex. $\Gamma = -8.7 \times 10^{-6}$ in the contour radially ahead of the vortex. Γ values are in $m^2 s^{-1}$.

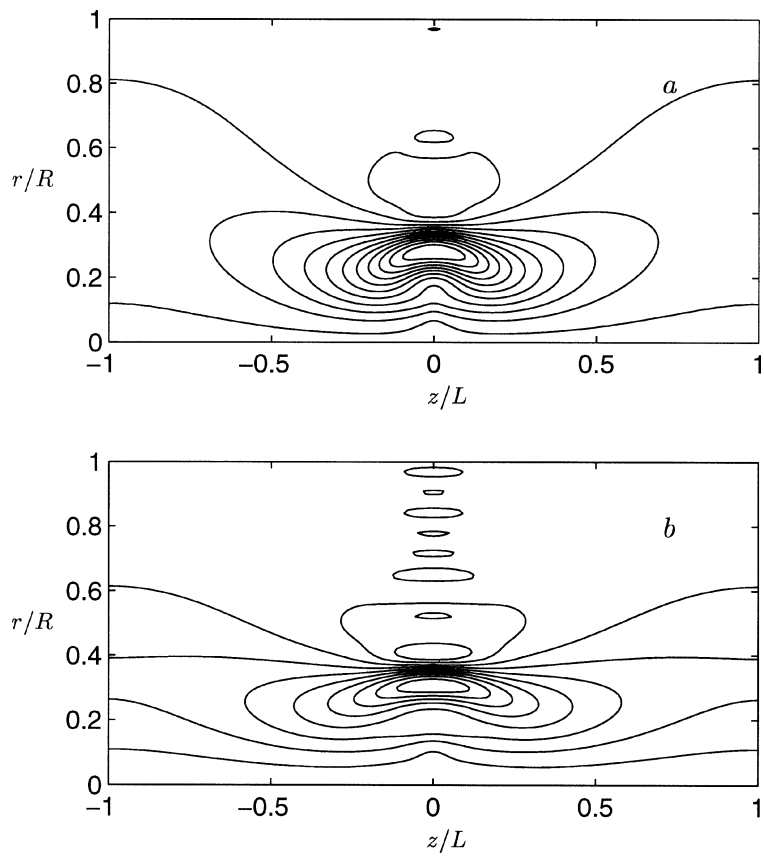

Figure 5. Contour plots of the Γ-field at $N_0 = 0.3$: (a) when $t/\tau = 3.0$, $\Gamma_{\max} = 1.8 \times 10^{-4}$ at $r \approx 0.3R$, and $\Gamma = 2.2 \times 10^{-5}$ at the outer contour of the vortex. $\Gamma = -1.2 \times 10^{-5}$ in the contour ahead of the vortex; (b) when $t/\tau = 7.5$, $\Gamma_{\max} = 1.3 \times 10^{-4}$ at $r = 0.3R$, $\Gamma = 3.4 \times 10^{-6}$ at the outer contour. In the region of reverse flow, $\Gamma = -1.94 \times 10^{-5}$. Γ values are in $m^2 s^{-1}$.

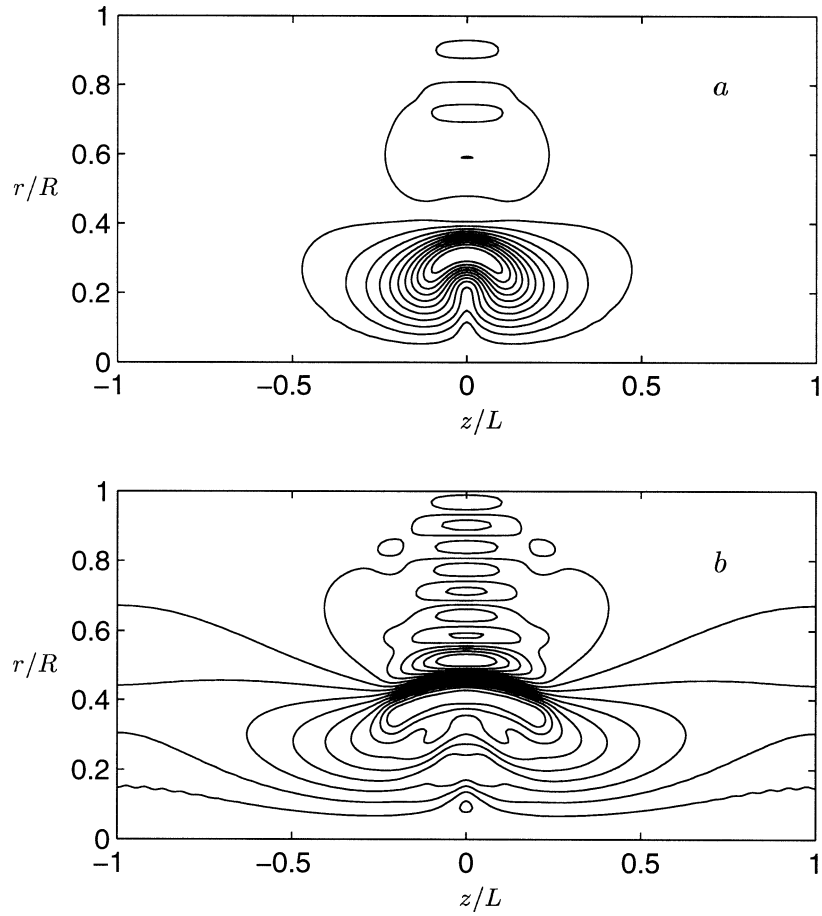

Figure 6. The Γ-field at $N_0 = 0.12$: (a) when $\tau = 1.0$, $\Gamma_{\max} = 2.4 \times 10^{-4}$ at $r \approx 0.3R$, and $\Gamma = 1.6 \times 10^{-5}$ at the outer contour of the vortex. $\Gamma = -5.7 \times 10^{-6}$ in the contour immediately ahead of the vortex; (b) when $t/\tau = 5.0$, $\Gamma_{\max} = 8.5 \times 10^{-5}$ at $r = 0.4R$. A high gradient in angular momentum exists at the front end of the vortex. Γ values are in $m^2 s^{-1}$.

a very weak magnetic field, there is a also a well-defined axial diffusion of Γ in addition to the radial transport. By stretching the Γ-lines in its direction, the magnetic field tries to reduce the gradients in Γ at the front end of the vortex.

Figure 7 shows the energy decay for different field strengths. As N_0 decreases, the decay rate becomes faster. When $N_0 = 10$, the evolution is purely linear. The energy decay is found to follow the law

$$\frac{E}{E_0} = \left[1 + 0.9(t/\tau)\right]^{-0.5} \tag{47}$$

until $t \approx 7\tau$. Beyond this time, the energy curves tend to go flat, showing that the current density in the core of the flow has fallen to a value that makes Joule dissipation small. Further evolution is not of much interest because the vortex feels the influence of the boundaries of the domain. When the parallel length scale of the growing vortex attains the size of the cavity, the velocity field is practically independent of the coordinate parallel to **B** and hence, by equation (16), the current density tends to zero. Due to the finite size of our domain, it would not be possible to begin with a high value of N_0 and observe the transition to a state when the inertial

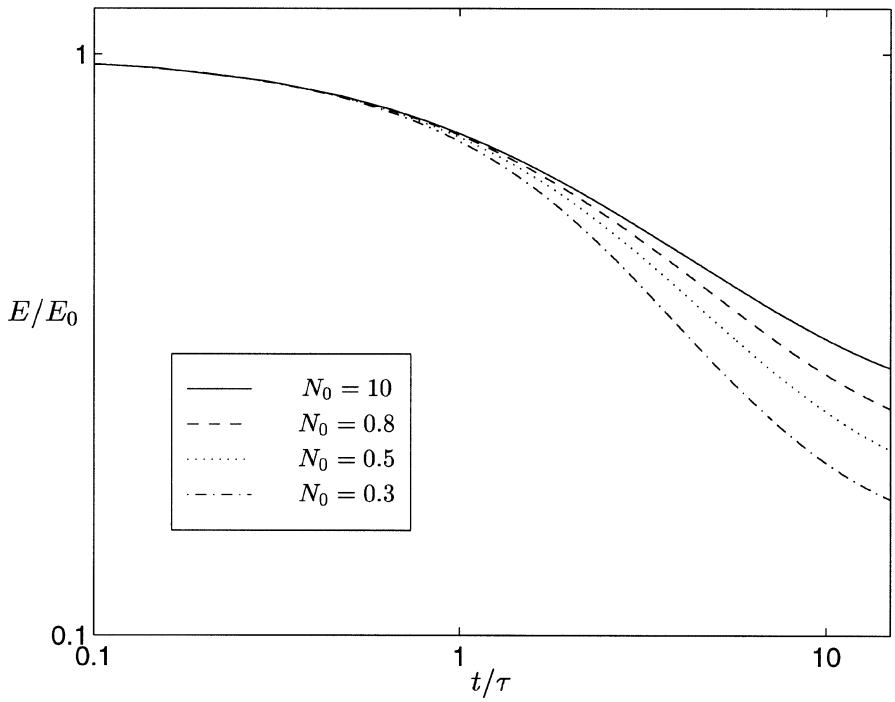

Figure 7. Decay of kinetic energy at different field strengths.

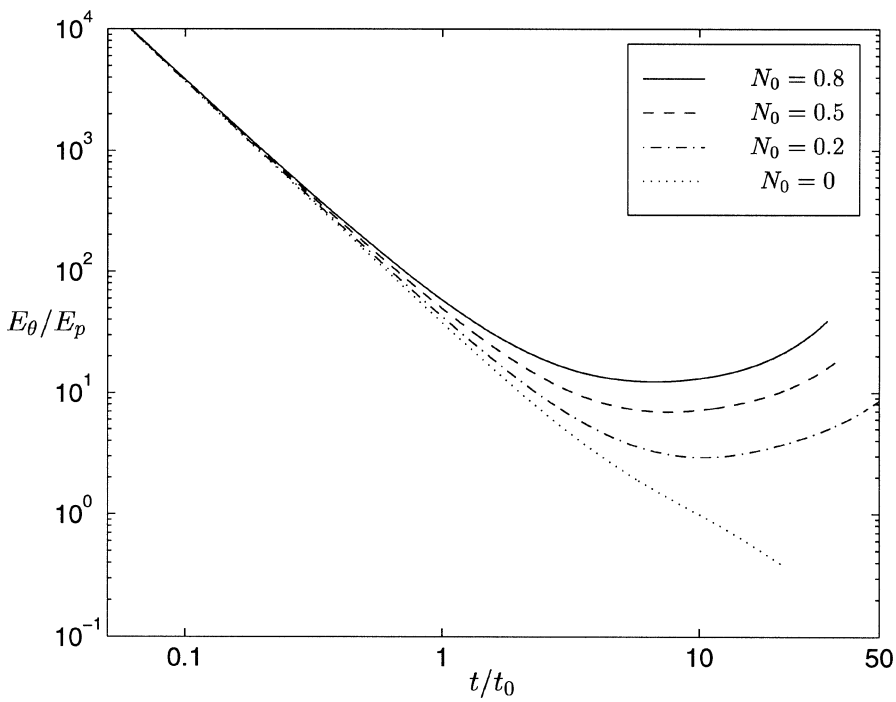

Figure 8. Ratio of toroidal to poloidal energies under strong, weak and zero fields. The curve rises after a minimum, indicating that E_p is damped faster than E_θ by the field.

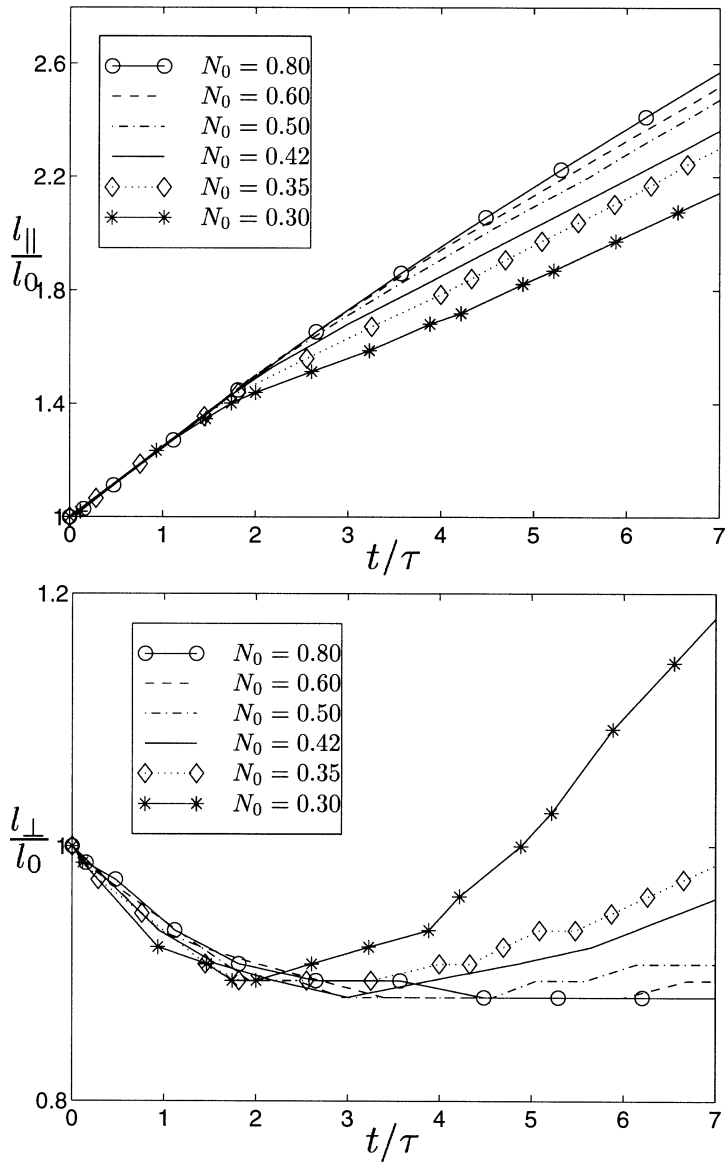

Figure 9. Variation of $l_{\|}$ and $l_{\perp}$ of a parallel vortex at different values of N_0.

and Lorentz forces balance. We, therefore, suitably reduce the value of N_0 in order to identify this state of equilibrium at $t = 0$. In view of this, we have focussed attention on interaction parameters of order unity.

Even if the viscous dissipation terms in the governing equations are dropped in the analysis, there is no visible change in the energy decay. This indicates that the contribution of viscosity to the overall energy dissipation is insignificant.

Figure 8 compares the ratio of the toroidal to the poloidal energies, E_θ/E_p, for different field strengths. The time axis is normalized with respect to the eddy turn-over time. $E_p = 0$ initially, but the ratio falls due to transfer of energy from E_θ to E_p as indicated by the first term on the right hand side of equation (39). A strong magnetic field arrests this transfer so that the maximum value of E_p is atleast one order of magnitude smaller

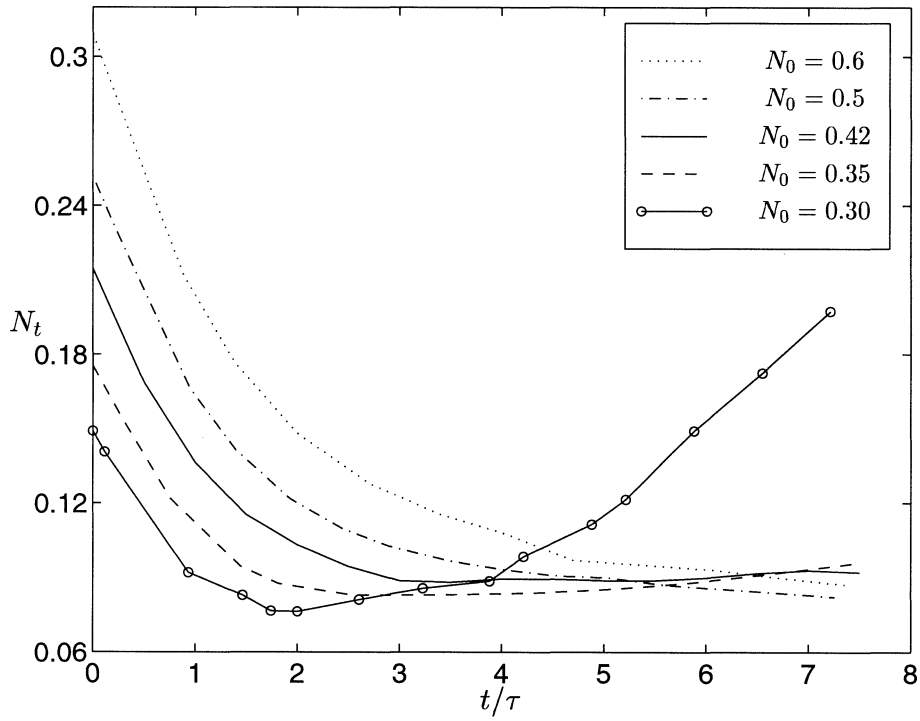

Figure 10. Variation of the true interaction parameter, N_t, at different field strengths.

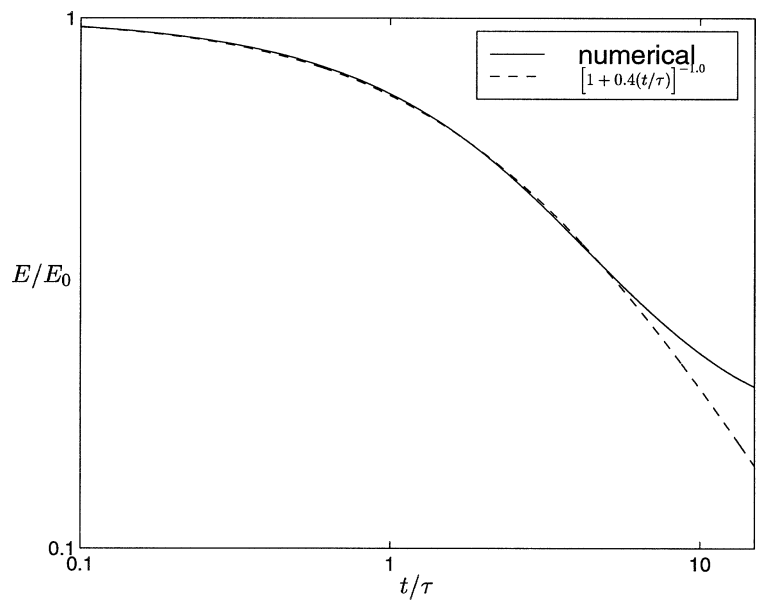

Figure 11. Comparison of the numerically-obtained energy decay with the theoretical estimate for $N_0 = 0.42$. The coefficient of (t/τ) is found to be 0.4.

than E_θ. A weaker field ($N_0 = 0.2$) allows greater transfer of energy, so that E_p is almost of order E_θ before Joule dissipation becomes important. For an undamped flow, E_p keeps building up at the expense of E_θ so that the energy ratio decreases continuously.

Figure 9 gives the parallel and perpendicular length scales at different values of N_0. As N_0 decreases, the rate of growth of $l_\parallel$ also decreases, implying weaker diffusion of Γ along the **B**-lines. When $N_0 = 0.8$, $l_\perp$ is approximately constant, barring the small initial contraction suffered by the vortex. As the field strength is reduced, an increase in the transverse length scale is observed. However, the increase of $l_\perp$ seen at $N_0 = 0.3$ does not represent the transverse growth of the vortex, but actually reflects the growing tendency of the vortex to form a ring that moves radially outward. This effect is more pronounced as the field becomes weaker. The definition of $l_\perp$ of the vortex does not hold good if $N_0 < 0.4$.

The behaviour of the true interaction parameter, N_t is shown in *figure 10*. The variation of N_t is studied by reducing the field strength gradually. For $N_0 > 0.4$, N_t decreases and tends to an approximately constant value around 0.1. For instance, when $N_0 = 0.5$, N_t decreases by 20% in the time range $3\tau < t < 7\tau$. When $N_0 = 0.42$, the value of N_t is nearly invariant in the same range. The initial decrease is attributed to the contraction in $l_\perp$ observed earlier. For a lower field strength, ($N_0 = 0.35$), N_t increases, but gradually (by about 12%) in the above time range. For lower values of N_0, the N_t values obtained will represent the unstable situation found earlier with the transverse length scale. This regime, where inertial forces dominate from $t = 0$, leads to an evolution of the kind seen in *figures 5* and *6*.

In short, when $N_0 > 0.4$, the Lorentz forces dominate initially, and the vortex will approach a state where magnetic and inertial forces balance. If $N_0 \approx 0.4$, the two forces are approximately of the same magnitude initially. This can be verified further by looking at the energy decay curve when $N_0 = 0.42$ (*figure 11*). The numerically-obtained energy decay is found to follow the law

$$\frac{E}{E_0} = \left[1 + 0.4(t/\tau)\right]^{-1} \tag{48}$$

until the evolution of the vortex is influenced by the presence of the boundaries normal to **B**. The velocity gradients in the direction of **B** are suppressed and consequently, the Joule dissipation falls. The above result indicates that, if the domain of evolution were infinite in extent, the global kinetic energy would decay as $(t/\tau)^{-1}$ at large times ($t \gg \tau$).

5. Discussion

In the present work, the evolution of an isolated vortex whose axis is parallel to the externally-applied steady magnetic field is investigated by an order-of-magnitude analysis as well as by a numerical model. The order-of-magnitude analysis for the non-linear evolution of a vortex, developed in section 3, rests on three ideas: (a) conservation of the component of the angular momentum parallel to the field, (b) conservation of energy and (c) the principal assumption that the true interaction parameter, N_t, is a constant of order unity if the inertial and Lorentz forces balance. The global evolution of a vortex at large N_0 comprises a linear phase in the range $\tau < t < N_0^2\tau$, wherein the energy decays as $(t/\tau)^{-1/2}$, and a subsequent non-linear phase wherein the energy decays as $(t/\tau)^{-1}$.

With the numerical model, we have performed a quantitative characterization of the evolution of a vortex under a moderate magnetic field. The interaction parameters considered are of order unity. This area has not yet received attention in the literature. An initially spherical vortex undergoes different structural changes depending on the field strength. Under a strong enough magnetic field, the dominant mechanism is diffusion

of angular momentum along the field lines. The behaviour under a weak magnetic field ($N_0 < 0.4$) is complex because the centrifugal forces acting on the vortex outweigh the Lorentz forces initially. While the structure propagates radially outward like a thermal plume, it also diffuses axially due to weak Joule dissipation.

The computational results show that the true interaction parameter can be used as a good index of the relative magnitudes of the magnetic and inertial forces above a certain field strength. When $N_0 > 0.4$, N_t is seen to converge to a finite value (*figure 10*), which indicates the beginning of a non-linear phase. If N_t is invariant in a given time range, it implies that the two forces are approximately of the same magnitude. In the present work, this condition is met when $N_0 \approx 0.4$. If $N_0 < 0.4$, we cannot expect N_t to tend asymptotically to a constant value. An unstable radial propagation created by dominant inertial forces takes place.

The numerical results obtained for $N_0 = 0.42$ support the order-of-magnitude investigation. First, our assumption that N_t is a constant in the non-linear regime is proven to be correct. Second, the numerically-obtained law of decay of kinetic energy agrees well with the analytical law, at finite time. Since the decay of the vortex is studied in a confined region, the long-time evolution will be influenced by the presence of boundaries. If the vortex were to evolve in an infinite domain, we can expect the energy to decay continuously as $(t/\tau)^{-1}$ at large times. From the point of view of studying the evolution at larger times, it is desirable to solve the problem in a larger domain and with a finer resolution. In such an analysis, a strong magnetic field could be imposed and the transition from the initial linear phase to the phase when N_t is a constant could be studied.

The contribution of viscosity to the overall damping of the vortex is found to be negligible. This is because the major contribution to the destruction of kinetic energy comes from Joule dissipation, a phenomenon that takes place at the large scales.

Acknowledgements

Binod Sreenivasan's work was supported by a Cambridge Nehru–Chevening scholarship and a Junior Research Fellowship from Hughes Hall, Cambridge.

References

[1] Votsish A.D., Kolesnikov Yu.B., Spatial correlation and vorticity in two dimensional homogeneous turbulence, Magnitnaya Gidrodinamika 11 (3) (1975) 25–28.
[2] Alemany A., Moreau R., Sulem P.L., Frisch U., Influence of an external magnetic field on homogeneous MHD turbulence, J. Méc. 18 (1979) 277–313.
[3] Sommeria J., Moreau R., Why, how and when, MHD turbulence becomes two dimensional, J. Fluid Mech. 118 (1982) 507–518.
[4] Moffatt H.K., On the suppression of turbulence by a uniform magnetic field, J. Fluid Mech. 28 (1967) 571–592.
[5] Davidson P.A., Magnetic damping of jets and vortices, J. Fluid Mech. 299 (1995) 153–186.
[6] Kolesnikov Yu.B., Tsinober A.B., Two-dimensional turbulent flow behind a circular cylinder, Magnitnaya Gidrodinamika 8 (3) (1972) 23–31.
[7] Sukoriansky S., Zilberman I., Branover H., Experimental studies of turbulence in mercury flows with transverse magnetic fields, Exp. Fluids 4 (1986) 11–16.
[8] Hinze J.O., Turbulence, McGraw-Hill, 1975.
[9] Purnir A., Siggia E.D., Development of singular solutions to the axisymmetric Euler equations, Phys. Fluids A 4 (1992) 1472–1491.
[10] Grauer R., Sideris T.C., Finite time singularities in ideal fluids with swirl, Physica D 88 (1995) 116–132.